Article

Urban Rainfall Anomaly under Intensive Development, 1949–2018, Case of Tel-Aviv, Israel

Pinhas Alpert [1,*], **Ronen Radian** [1], **Noam Halfon** [1,2] **and Zev Levin** [1]

1   Department of Geophysics, Faculty of Exact Sciences, Tel-Aviv University, Tel Aviv 69978, Israel;
    ronenrad@bezeqint.net (R.R.); noam.halfon@gmail.com (N.H.); zevlev@post.tau.ac.il (Z.L.)
2   Israel Meteorological Service, Bet-Dagan 5025001, Israel
*   Correspondence: pinhas@post.tau.ac.il; Tel.: +972-(0)-52-608-8364

Abstract: The primary objective here is the study of the urban rainfall anomaly patterns, particularly the positive/negative dipole reported in the literature as well as their temporal/spatial evolution due to rapid urban development. The spatial changes in the annual rainfall distribution, eastward and downwind of the largest coastal urban area of Israel, i.e., the Greater Tel Aviv region, in relation to the rapid expansion of the urban area are analyzed. This provides a unique opportunity, as shown here, to study the effect of a most rapid urban expansion on the potential for urban rainfall anomalies. Tel-Aviv probably serves as a case study for other fast-growing Mediterranean cities. Rain gauges' data (over 100) collected over a period of 70 years (1948–2018), are divided into six sub-periods of 20 years and plotted on top of the urban area growth in those years. The average precipitation spatial distributions and their anomalies are both calculated for each sub-period. The results were examined along three geographic lines of particularly rapid urban expansion over the area, towards the northeast, east, and southeast. Increases of the precipitation downwind of the urban area are noticed when progressing along with the urban development. In addition, an upwind decrease over the coastal region is found. These findings are well correlated with the expansion of the urban area and the rainfall urban anomalies, P_{dev}, are of the order of 50–100 mm/y. Other potential explanations to these anomalies are discussed and suggested to be less feasible.

Keywords: urban rainfall; Greater Tel Aviv area; Mediterranean climate; urbanization

1. Introduction

The contribution of urban areas to the formation and/or modification of precipitation has been noted in several studies over Israel, with a focus on the increase in annual precipitation caused by the urbanization of the Greater Tel Aviv region. Goldreich and Manes (1979) [1] showed that the annual rainfall at stations within the boundaries of the Tel-Aviv metropolitan area as well as in downwind regions exhibit increasing trends with respect to stations outside of these boundaries. They suggested the urban heat island (UHI) as the main factor. Stanhill and Rapaport (1988) [2] found, however, that the total amount of precipitation over Israel has not changed despite the expansion of the urban area and therefore concluded that urbanization does not change the overall amount of precipitation, only its spatial distribution. Shafir and Alpert (1990) [3] found a positive urban precipitation anomaly in Jerusalem employing a simplified 2-D terrain following model. Givati and Rosenfeld (2004) [4] have suggested that "urban air pollution and industrial air pollution have been shown qualitatively to suppress rain and snow." Alpert et al. (2008) [5], however, rejected their methodology of employing an orographic rainfall ratio and called for further studies. Halfon et al. (2009) [6] found significant increases in annual rainfall downwind of the greater Tel-Aviv area.

There are four primary factors that may modify precipitation over urban areas as listed by Oke (1979) [7], Landsberg (1981) [8], and Shepherd (2005) [9]. These factors are: (a) The UHI, which increases urban air instability; (b) absolute humidity, which can be higher or lower; (c) urban roughness, which enhances wind convergence and consequently the mechanical convection; and (d) air pollution, which may act as cloud condensation nuclei (CCN) or ice nuclei (IN). The latter effect depends on the urban aerosol types and consequently the concentration of those nuclei may increase or decrease the amount of precipitation. Van den Heever and Cotton (2007) [10], for instance, suggested that urban-forced convergence downwind of the city, rather than the presence of greater aerosol concentrations, determine whether storms actually develop in the downwind region. Once convection is initiated, urban-enhanced aerosols can exert a significant effect on the dynamics, microphysics, and precipitation produced by these storms. However, the response to urban-enhanced aerosols depends on the background concentrations of aerosols; a weaker response to urban aerosols occurs with increasing background aerosol concentrations, as shown by Teller and Levin (2006) [11]. In a subsequent study, Van den Heever et al. (2011) [12] employed factor separation methodology to highlight the important role of synergies among the different urban factors. In addition, if urban air pollution includes giant aerosols, there definitely could be an increase in rainfall (Levin and Cotton, 2009) [13].

The aforementioned urban factors obviously depend on the season and type of synoptic events, which can modify the precipitation above the city area or in its vicinity. Bornstein and Lin (2000) [14] and Shepherd (2005) showed that the UHI has a major contribution to the convection or generation of thunderstorms and enhances the hot-season precipitation. Bornstein and Johnson (1997) [15] showed that high wind speed (above 4 m/s) may inhibit the UHI formation. Gaffen and Bornstein (1988) [16] showed that a slow moving synoptic scale cold front was highly distorted as it passed through New-York City due to friction. Most of the case studies were in hot and wet seasons while fewer were performed in the relatively cold wet winter with passages of cyclonic storms, like in the Mediterranean and particularly in the present study area of Tel Aviv. Terjung et al (1971) [17] showed that during storms, the frontal passage caused a reduction of 92% in the absorbed solar radiation. On a cold winter day, when the synoptic wind is stronger, the wind-induced vertical motion upwind may generate precipitating clouds over city areas while a weaker UHI, if present, may contribute to clouds' formation and precipitation downwind of the urban area.

Israel's climate is typified by hot/dry summers and cool/wet winters, typical for the Mediterranean climate. The precipitation season extends from September to May, and over 90% of the total precipitation falls during October–March (Goldreich, 2003) [18]. Based on the IMS (Israel Meteorological Service) data, the average maximum surface temperatures near the Tel-Aviv coast are 19 °C in December, 17.5 °C in January, and 17.8 °C in February. The average daily surface temperatures in winter are of the order 13–14 °C while coastal SSTs (sea surface temperature) vary from 18 °C in December to a minimum of ~16 °C in February. Hence, by comparing the land to SSTs, it can be assumed the UHI effect is secondary.

Winter precipitation systems are commonly associated with a mid-tropospheric trough over the Mediterranean sea, west of Israel, and low level cyclones somewhere between the Turkish coast, such as Antalya Bay to an area west of Gaza (Figure 1). These systems yield about 90% of the annual precipitation over Israel (Shay-El and Alpert 1991 [19]). On average, the wind during rain has a westerly component (Alpert and Shay-el, 1994 [20]). Most of the precipitation falls with the SW-W wind direction sector due to the associated longer path over sea, cold front convergence, and higher wind speeds. The absolute humidity strongly depends upon the SSTs and the air layer above it. The longer the path of the air parcels above the sea, the higher the humidity is. As the air moves inland away from the coast, the surface humidity generally drops. Hence, the development of clouds inland is strongly dependent on the wind direction and speed. Since most winter precipitation systems are frontal cold cyclones, the majority of these systems are characterized by conditional instability (Alpert and Reisin, 1986 [21]), so that urban mechanical convection is an important factor for clouds'

formation. As to coastal effects, wind convergence due to a roughness change causes an air uplift that may initiate convection and cloud formation. The contribution of this effect to precipitation is evident a few km downwind of the coast and may add to urban effects. This effect of convection and cloud formation due to coastal roughness was also noticed in summer morning coastal cloudiness (Alpert and Getenio, 1988 [22]).
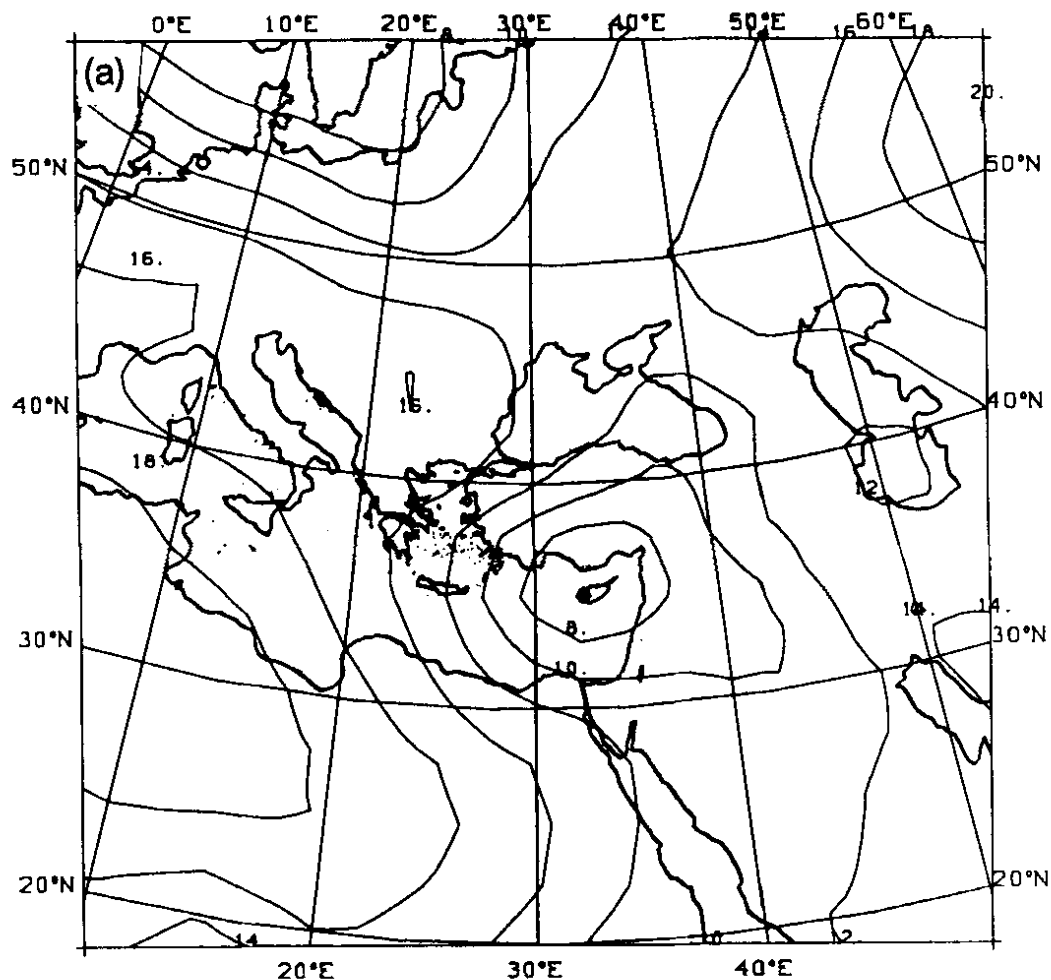

Figure 1. Composite Cyprus low of 1000 hPa (hectopascal = mb) geopotential height (2 dam interval); from Shay-El and Alpert, 1991 [19].

During the last 60 years, a large variability of rain over Israel was found. In the 1950s, there was a long drought, while the 1960s and 1970s were relatively wet. These years were followed by a trend of rain reductions over the region, particularly in recent years, with some outstanding blessed years, like 1992 and 2003, or dry ones, like 1998 and 2008. Changes in the frequency of Cyprus cyclones, mainly spring reductions, were noticed (Alpert et al. 2004 [23]). No significant changes have been noticed in the overall structure either of the synoptic system or in the wind direction. None of these changes, however, could explain the trend of the eastward moving urban rainfall anomaly discussed in the present paper. In contrast, we may have expected an inland rainfall reduction due to some weakening of the Cyprus cyclones (Alpert et al. 2004 [23]). This drying trend was recently shown to be enhanced during the 21st century due to global warming effects [24–26].

Halfon (2008) [27] found no significant temporal change of the all-Israel average annual rainfall. There are, however, small regional changes in rainfall amounts downwind to the coastal cities and a slight decrease of precipitation over the east High Galilee Mountains. Ziv et al (2013) [28] analyzed the 1975–2010 trends and found a significant decrease of precipitation over the arid areas mostly over

southern Israel. Also, a trend of a slight decrease of precipitation over Israel and a shorter precipitation season was identified.

The primary objective here is to study the urban rainfall anomaly patterns, particularly the positive/negative dipole reported in the literature as well as their temporal/spatial evolution due to rapid urban development. This expansion is expressed by both the increase in the urban area and the increase of high buildings changing the surface roughness.

2. The Study Area

The Tel Aviv topography is a nearly flat sandy plane in the proximity of the sea with low hills (~10 s of m) to the east with mostly agricultural fields. Table 1 shows the population of the Greater Tel-Aviv municipality since 1949. The expansion of the urban area of Tel Aviv city itself was fast and reached a maximum in the early 1960 s. The development of the other municipalities in the inner-first ring (Figure 2) continued eastward. Figure 2 shows the geography of the municipalities in the kernel (zone 1), first ring (zone 2), and second ring (zone 3). As to changes in the roughness of the Greater Tel-Aviv urban area, Table 2 summarizes the numbers of high tower buildings built over the years. In the 1950s, first buildings higher than 4–6 floors were built mainly along the seashore. In 1965, the first sky scraper was built with 34 floors (Table 2, above 30 floors). The building of high towers has accelerated from 1968 till present.

Table 1. Population of the municipalities of the Greater Tel Aviv area ("Gush-Dan") during 1948–2008 from annual statistics of Israel (central bureau of statistics) for the years of 1948–2008. Other "second ring" municipalities (not mentioned in the table) that become significant since 1980 are: Efal, Kiryat-Ono, Or-Yehuda, and Yehud-Monosson (Figure 2). Population densities in 2008 vary from 1770 p/km^2 in Tel-Aviv municipality to 15,000 p/km^2 in Bat-Yam and 21,000 p/km^2 in Bnei-Brak. The last two, i.e., Bat-Yam and Bnei-Brak, are the densest in Israel.

Year		1948	1958	1968	1978	1988	1998	2008
Municipality								
Kernel (zone 1 in Figure)	Tel Aviv-Jaffa	248,260	383,000	384,700	339,800	317,000	348,000	392,000
First ring (zone 2 in Figure)	Giv'atayim	9635	26,000	42,000	49,000	45,600	46,800	49,900
	Ramat-Gan	17,182	77,000	109,400	120,300	115,700	126,900	134,000
	Bnei-Brak	8834	36,600	67,000	87,300	109,400	133,900	153,000
	Holon	9568	40,000	80,000	124,500	146,000	163,000	170,000
	Bat-Yam	2331	21,000	68,900	126,000	133,000	137,000	129,000
Second ring (zone 3 in Figure)	Petah Tikva	21,589	49,000	76,700	114,400	133,600	160,000	193,000
	Rishon-Lezion	10,445	24,000	42,000	83,400	123,000	188,000	226,000

Table 2. Number of tower buildings in Greater Tel-Aviv area; according to number of floors; 6–15, 15–30, and >30 floors, following Margalit (2001) [29]. The tower buildings in the Table were built in the Greater Tel-Aviv area since 1953, during the pertinent period.

Period	1953–1967	1968–1977	1978–1988	1989–2001
6–15 floors	68	269	127	256
15–30 floors	3	20	33	37
>30 floors	1	0	1	6

Figure 2. Municipalities of Greater Tel- Aviv area. The kernel zone (denoted 1) is Tel-Aviv-Jaffa (Jaffa Harbor is denoted by the red point at 32.03 N, 34.45 E). First and second rings municipalities are listed in Table 1 and are denoted here by zones 2 and 3, respectively. The other municipalities indicated to the north are not considered part of Greater Tel-Aviv in this study.

3. Data and Methods

3.1. The Rainfall Data

The study region consists of a rectangle confined by latitudes 31°45′–32°15′ N and longitudes 34°40′ N–35°20′ E, Figure 3. The location of Tel Aviv center (X in Figure 3) was determined by the half-way distance between the N–S and E–W boundaries of region 1 in Figure 2. A detailed list of the stations can be found in Halfon (2008) [27]. The daily precipitation measurements are from about 100 rain gauges stations over the study area, received from the Israel meteorological service (IMS), that were operational in each pertinent study period, Figure 3. The IMS routinely maintains and calibrates the rain gauges and the data were measured by standard gauges, which have an accuracy of 1%–2%.

Figure 3. The study area and the Israel Meteorological Service (IMS) rain stations (over 100 stations, denoted by circles) employed here. The study area is indicated by the red rectangle. For more detail see text. Tel-Aviv city center is located at about (32°04′ N, 34°47′ E), and is denoted by an X.

3.2. The Urban Area

Maps of the urban area for each sub period were plotted based upon data from the "Israeli National Agency for Mapping and Geographic Information" (Ref MAPI [30]). The average precipitation over the whole research area (Figure 3, Red Rectangle spatial mean) and for each sub-period were computed. Next, the areal rainfall deviation, P_{dev}, from the averages between the long term average annual precipitation of each station to the long term areal average were calculated. The P_{dev} field was mapped over the urban area of the greater Tel Aviv region for each sub-period, Figure 4. Detailed description of the rainfall interpolation methodology can be found in Halfon et al. (2009) [31].

Three geographic lines (rays) were chosen along the densest expansions of the urban areas (Figure 5) and the rain anomalies for the last five periods vs. the distance from the coast along the rays are plotted in Figure 5.
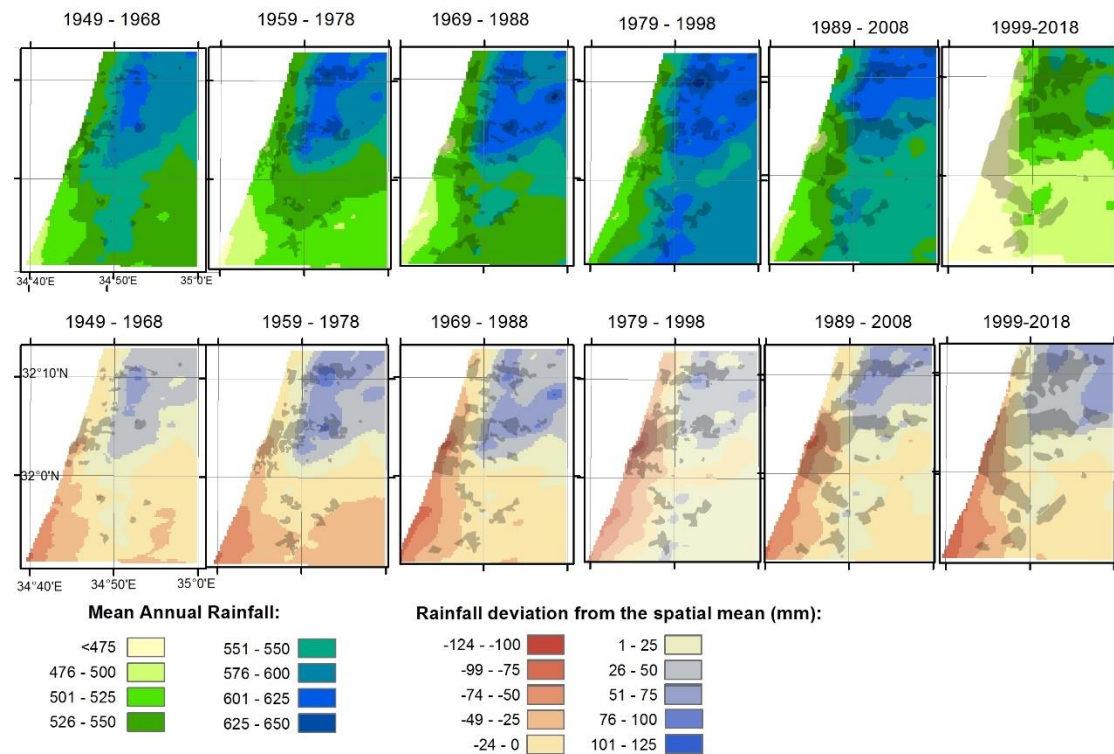
Figure 4. Upper panels: the annual precipitation means for the six sub-periods superimposed over the changing urban area (shaded). Lower panels show the rainfall deviation, P_{dev}, from the mean areal average over urban area. The enhanced positive/negative dipole can be noticed to be progressing inland along with the urban development. Rainfall (upper panels) and rainfall deviations (lower panels) color bars are given at the bottom.
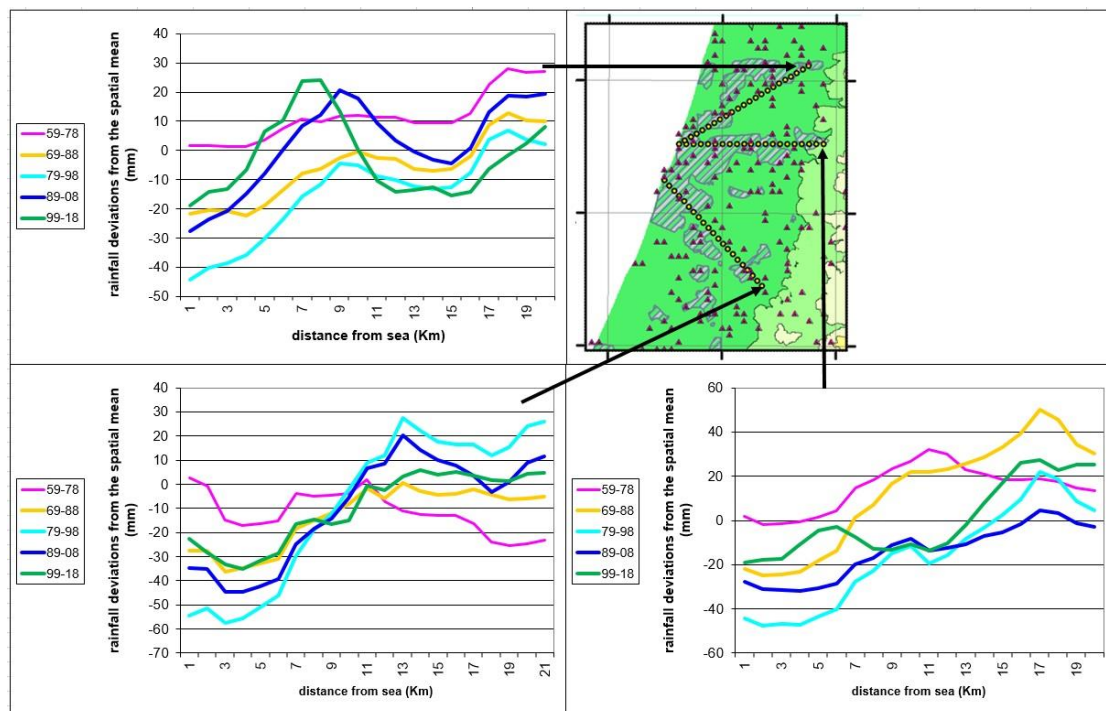

Figure 5. Three geographic lines (or rays) pointing over the greater Tel-Aviv urban area expansion and the corresponding precipitation anomalies for the five chosen 20-year sub-periods, i.e., 1959–1978, 1969–1988, 1979–1998, 1989–2008, and 1999–2018. Upper-right panel urban areas and stations (in triangles) correspond

to the most-recent sub-period of 1999–2018. The urban shading is added here with inclined lines and shading (same as the black areas in Figure 4) is shown as well as the geographic location of the three rays over the densest urban areas, as defined by the built-up area. The three panels, one for each ray, show the rainfall anomalies, P_{dev}, relative to the average areal annual precipitation, for the five sub-periods from 1959 to 2018 vs. the distance from the sea-shore (km).

4. Results

The full study period of 1949–2018 was divided into six partially overlapping sub-periods of 20-year, as follows; 1949–1968, 1959–1978, 1969–1988, 1979–1998, 1989–2008, and 1999–2018. This was done, following different sub-divisions of periods, in order to smooth short period fluctuations, which could be due to sub decadal or other inter-annual variation. The 20-year averaging period was chosen following the early examination of other smaller sub-periods, like 10-years, in which the rainfall maps were found to be too noisy. The upper panels of Figure 4 show the annual precipitation means for the five sub-periods plotted over the pertinent maps (for each sub-period) of the urban area (shaded). The bottom panels show the deviations from the mean over the urban area (shaded-violet). Figure 4 illustrates that as the built-up area has expanded eastward with time, the precipitation deviation (i.e., P_{dev}) near the sea-shore becomes increasingly negative; while downwind to the built-up area, i.e., 9–17 km eastward, P_{dev} becomes increasingly positive. This demonstrates that the enhanced positive/negative dipole progresses inland along with the urban area development.

Figure 5 in its upper right panel shows the three geographically expansion lines over the primary densest (defined here in the sense of building density) urban development of Greater Tel-Aviv along with three panels, one for each line/ray. Notice that the first period, 1949–1969, was omitted because six lines were too dense for the figures and its contribution was small. As the urban area expands, the negative rain deviation near the seashore (~0–9km) develops and the positive anomaly moves inland at about 9–17 km from the coast line.

The primary finding is that as the urban area expands with time, the deviations near the sea-shore progress inland along the three expansion lines. One should note that the graphs present the rainfall anomalies from the spatial mean (Figure 3, red rectangle) of the precipitation over the study region such that the lines should be analyzed according to the changes along the distance downwind.

It should be noted that the most recent relatively drier period of 1999–2018 (as pointed out by, e.g., Ziv et al. 2013 [28]) does show a weaker rainfall dipole (Figures 4 and 5). This is not surprising since drier years are also reflected in the reduced urban effect. This is evident in Figure 5 (green line) in which the positive rainfall anomaly is reduced for this period for all three urban expansion lines.

5. Discussion

During the last 70 years, changes have not been large enough to be noticed in the overall structure of neither the synoptic systems or in the wind direction that may explain the presented large 20-year average urban rainfall dipole. This seems to be the case for the Tel Aviv urban scale, which is smaller compared to changes in the synoptic patterns that were discussed with a daily resolution (Hochman et al. 2018 [24], Alpert et al. 2008 [5], Halfon et al. 2009 [6]). The trends of the Cyprus lows to become shallower were noticed along with some southern movement of the cyclones' centers. These changes, however, do not seem strong enough to explain the significant eastward shift of the Greater Tel Aviv urban rainfall anomalies.

It is interesting to note that an earlier similar study followed the METROMEX project in St. Louis, Changnon et al. (1971) [31]. This study does not show the same detail of the urban development, but it does show an increase in rainfall downwind of the city with time as the city grew. The current findings are in agreement with other previous studies during the recent decades. The city of Tel Aviv was established in 1909, and since 1948, the Greater Tel Aviv urban areas have undergone intensive development and have significantly expanded from the Mediterranean seashore eastward. The current 70-year study period and the relatively large number and density of stations (>100) that were employed here, allowed us to suggest a strong association between the urban growth and the pattern of the

precipitation dipole along the three primary inland expansion lines of Greater Tel Aviv. As to the dominant physical mechanism, it was noticed that the main rainy season in Israel is the cold winter, and most of the rainfall events in the Tel-Aviv area are associated with cold frontal cyclones and typical winds from the west sector arriving from the Mediterranean Sea with speeds often exceeding ~5 m s^{-1}. Since the average-maximum urban temperature is of the same order of the SST, the storm wind speed interaction with the urban roughness and friction seems to be the more dominant mechanism as compared to the UHI effect. Furthermore, Carrio et al.'s (2010) [32] results reinforce the conclusion of the dominance of urban land-use effects vs. aerosols. A global tendency of an increase in UHI was recently shown employing MODIS (MODerate resolution Imaging Spectroradiometer satellite data for the summer period (Itzhak-Ben-Shalom et al. 2017 [33]).

We should stress that if the assumption that the urban roughness is the more dominant mechanism (as compared to the UHI effect) is correct, then the UHI effect would become stronger at the end of the season (March–April), when the land temperature rises, while the SST remains relatively low. This assumption, however, needs further research on the seasonal rainfall variations, which are beyond the scope of the present study.

6. Conclusions

The primary objective here was the study of urban rainfall anomaly patterns, particularly the positive/negative dipole reported in the literature as well as their temporal/spatial evolution as associated with rapid urban development. The practical implications are for better quantification of climatic rainfall variations in the proximity of urban areas since urban changes are quite significant and should therefore be taken in account. This is of particular interest in an area which has undergone significant climate variations in recent decades and in such proximity to an arid and semi-arid zones just south of Tel Aviv ($\leq$100 km).

It was shown here that positive (increase) trends in the 20-year running average rainfall anomalies downwind of the urban area of greater Tel Aviv along with negative (decrease) trends near the coastal strip tend to be progressing with time inland since 1949 until 2018. This average rainfall anomaly dipole was shown to progress inland along with the associated urban area expansion eastward.

The conclusion about the roughness dominance over UHI requires an associated modeling study that will help resolve the contribution of each factor and evaluate its relative contribution to the observed changes in the spatial distribution of precipitation along with the effects of potential synergies among the factors. It is our intention to perform such simulations employing the factor separation approach of Alpert and Sholokhman (2011) [34]. Using the factor separation to separate these three variables, i.e., UHI, roughness, and aerosols, is difficult, but very important. For the aerosols, one can use two extreme cases of a clean and pollution case in which rain was present. Another possibility is to use, instead of real cases, artificial ones. Namely, the conditions of a rainy day are taken and two extreme values of pollution are used while the other factors remain the same, namely the UHI and the roughness. Modelling of all potential urban effects in a very realistic way is beyond the scope of this paper. For instance, we recently performed daily low-resolution forecasts of sea-salt aerosols over the Mediterranean area, aerosols that are quite abundant in the Tel Aviv coastal area (Kishcha et al. 2011) [35] as well as daily prediction of dust aerosols (Alpert et al. 2002 [36]). However, their effects on clouds and rainfall as well as the real effects of the other types of urban aerosols require very high resolutions (well below ~1 km) and are still under intensive research (Levin and Cotton, 2009 [13]).

Conflicts of Interest: The authors declare no conflict of interest.

References

1.　Goldreich, Y.; Manes, A. Urban effects on precipitation patterns in the greater Tel-Aviv area. *Theor. Appl. Climato.* **1979**, *27*, 213–224.

2.　Stanhill, G.; Rapaport, C. Temporal and Spatial Variation in the Volume of Rain Falling Annually in Israel. *Isr. J. Earth Sci.* **1988**, *37*, 211–221.

3.　Shafir, H.; Alpert, P. On the urban orographic rainfall anomaly in Jerusalem—A numerical study. *Atmos. Environ.* **1990**, *3*, 365–375. [CrossRef]

4.　Givati, A.; Rosenfeld, D. Quantifying Precipitation Suppression Due to Air Pollution. *J. Appl. Meteorol.* **2004**, *43*, 1038–1056. [CrossRef]

5.　Alpert, P.; Halfon, N.; Levin, Z. Does air pollution really suppress precipitation in Israel. *J. Appl. Meteorol. Climatol.* **2008**, *47*, 933–943. [CrossRef]

6.　Halfon, N.; Levin, Z.; Alpert, P. Temporal rainfall fluctuations in Israel and their possible link to urban and air pollution effects. *Environ. Res. Lett.* **2009**, *4*. [CrossRef]

7.　Oke, T.R. *Review of Urban Climatology, 1973–1976*; WMO Technical Note No. 169; WMO: Geneva, Switzerland, 1979; p. 539.

8.　Landsberg, H. *The Urban Climate*; Academic Press: New York, NY, USA, 1981.

9.　Shepherd, J.M. A Review of Current Investigations of Urban-Induced Rainfall and Recommendations for the Future. *Earth Interact.* **2005**, *9*, 1. [CrossRef]

10.　Van den Heever, S.C.; Cotton, W.R. Urban aerosol impacts on downwind convective storms. *J. Appl. Meteorol. Climatol.* **2007**, *46*, 828–850. [CrossRef]

11.　Teller, A.; Levin, Z. The effects of aerosols on precipitation and dimensions of subtropical clouds: A sensitivity study using a numerical cloud model. *Atmos. Chem. Phys.* **2006**, *6*, 67–80. [CrossRef]

12.　Van der Heever, S.C.; Rozoffand, C.; Cotton, W.R. *Experience in Applying the Alpert-Stein Factor Separation Methodology to Assessing Urban Land-Use and Aerosol Impacts on Precipitation, in Factor Separation in the Atmosphere Application with Future Prospects*; Alpert, P., Sholokhman, T., Eds.; Cambridge University Press: Cambridge, UK, 2011; pp. 120–145, 274.

13.　Levin, Z.; Cotton, W.R. *Aerosol Pollution Impact on Precipitation: A Scientific Review*; Springer: Berlin, Germany, 2009; p. 386.

14.　Bornstein, R.D.; Lin, Q. Urban heat islands and summertime convective thunderstorms in Atlanta: Three cases studies. *Atmos. Environ.* **2000**, *34*, 507–516. [CrossRef]

15.　Bornstein, R.D.; Johnson, D.S. Urban-rural wind velocity differences. *Atmos. Environ.* **1997**, *11*, 597–604. [CrossRef]

16.　Gaffen, D.; Bornstein, R.D. Case Study of Urban Interactions with a Synoptic Scale Cold Front. *Meteorol. Atmos. Phys.* **1988**, *38*, 185–194. [CrossRef]

17.　Terjung, W.H. The effect of a cyclonic storm on the energy fluxes at the urban interface—A preliminary experiment. Arch. *Meteorol. Geophys. Biokl. Ser. B* **1971**, *19*, 367–416. [CrossRef]

18.　Goldreich, Y. *The Climate of Israel: Observation, Research and Application*; Kluwer Academic Publishes: New York, NY, USA, 2003.

19.　Shay-El, Y.; Alpert, P. A diagnostic study of winter diabatic heating in the Mediterranean in relation with cyclones. *Quart. J. R. Meteor. Soc.* **1991**, *117*, 715–747. [CrossRef]

20.　Alpert, P.; Shay-El, Y. The moisture source for the winter cyclones in the Eastern Mediterranean. *Isr. Meteor. Res. Pap.* **1994**, *5*, 20–27.

21.　Alpert, P.; Reisin, T. An early winter polar air mass penetration to the eastern Mediterranean. *Mon. Wea. Rev.* **1986**, *114*, 1411–1418. [CrossRef]

22.　Alpert, P.; Getenio, B. One-level modelling for diagnosing surface winds over complex terrain. Part I: Comparison with 3-D modelling in Israel. *Mon.Rev. Wea.* **1988**, *116*, 2025–2046. [CrossRef]

23. Alpert, P.; Osetinsky, I.; Ziv, B.; Shafir, H. Semi-objective classification for daily synoptic systems: Application to the Eastern Mediterranean climate change. *Int. J. Climatol.* **2004**, *24*, 1001–1011. [CrossRef]

24. Hochman, A.; Bucchignani, E.; Gershtein, G.; Krichak, S.O.; Alpert, P.; Levi, Y.; Yosef, Y.; Carmona, Y.; Breitgand, J.; Mercoglianoc, P.; et al. Evaluation of regional COSMO-CLM climate simulations over the Eastern Mediterranean for the period 1979–2011. *Int. J. Climatol.* **2018**, *38*, 1161–1176. [CrossRef]

25. Hochman, A.; Harpaz, T.; Saaronia, H.; Alpert, P. Synoptic classification in 21st century CMIP5 predictions over the Eastern Mediterranean with focus on cyclones. *Int. J. Climatol.* **2018**, *38*, 1476–1483. [CrossRef]

26. Samuels, R.; Hochman, A.; Baharad, A.; Givati, A.; Levi, Y.; Yosef, Y.; Saaroni, H.; Ziv, B.; Harpaza, T.; Alpert, P. Evaluation and projection of extreme precipitation indices in the Eastern Mediterranean based on CMIP5 multi-model ensemble. *Int. J. Clim.* **2017**, *11*. [CrossRef]

27. Halfon, N. Spatial Patterns of Precipitation in Israel and Their Synoptic Characteristics. Ph.D. Thesis, Haifa University, Haifa, Israel, 2008.

28. Ziv, B.; Saaroni, H.; Pargament, R.; Harpaz, T.; Alpert, P. Trends in Rainfall Regime over Israel, 1975–2010, and their Relationship to Large-Scale Variability. *Reg. Environ. Changes* **2013**, *14*. [CrossRef]

29. Margalit, T. High Rise Building in Tel-Aviv 1953–2001—A Politics of "Random" Order. Ph.D. Thesis, Tel-Aviv University, Tel Aviv, Israel, 2001.

30. MAPI. Available online: http://mapi.gov.il/en/Pages/default.aspx (accessed on 5 March 2019).

31. Changnon, S.A., Jr.; Huff, F.A.; Semonin, R.G. MTROMEX: An investigation of inadvertent weather modification. *Bull. Amer. Met. Soc.* **1971**, *52*, 958–968. [CrossRef]

32. Carri´o, G.G.; Cotton, W.R.; Cheng, W.Y.Y. Urban growth and aerosol effects on convection over Houston, Part I: the August 2000 case. *Atmos. Res.* **2010**, *96*, 560–574.

33. Itzhak-Ben-Shalom, H.; Alpert, P.; Potchter, O.; Samuels, R. MODIS summer SUHI cross-sections anomalies over the megacities of the monsoon Asia region and global trends. *Open Atmos. Sci. J.* **2017**, *11*, 121–136. [CrossRef]

34. Alpert, P.; Sholokhman, T. *Factor Separation in the Atmosphere, Applications and Future Prospects*; Cambridge University Press: Cambridge, UK, 2011; p. 274.

35. Kishcha, P.; Nickovic, S.; Starobinets, B.; di Sarra, A.; Udisti, R.; Becagli, S.; Sferlazzo, D.; Bommarito, C.; Alpert, P. Sea-salt aerosol forecasts compared with daily measurements at the island of Lampedusa. *Atmos. Res.* **2011**, *100*, 28–35. [CrossRef]

36. Alpert, P.; Krichak, S.O.; Tsidulko, M.; Shafir, H.; Joseph, J.H. A dust prediction system with TOMS initialization. *Mon. Wea. Rev.* **2002**, *130*, 2335–2345. [CrossRef]